Korean J Physiol Pharmacol
Vol 6: 173–181, August, 2002

The Gradient Model of the Rabbit Sinoatrial Node

H. Dobrzynski[1], M. Lei[2], S.A. Jones[1], M.K. Lancaster[1], and M.R. Boyett[1]

[1]School of Biomedical Sciences, University of Leeds, Leeds LS2 9JT, UK; [2]University Laboratory of Physiology, University of Oxford, Oxford OX1 3PT, UK

The sinoatrial (SA) node is a complex and inhomogeneous tissue in terms of cell morphology and electrical activity. There are two models of the cellular organisation of the sinoatrial node: the gradient and mosaic models. According to the gradient model there is a gradual transition in morphology and electrical properties of SA node cells from the centre to the periphery of the SA node. In the mosaic model, there is a variable mix of atrial and sinoatrial node cells from the centre to the periphery. This review focuses on the cellular organisation of the rabbit sinoatrial node in terms of the expression of connexin (Cx40, Cx43 and Cx45), L-type Ca^{2+} channel and Na^{+}-Ca^{2+} exchanger proteins. These immunocytochemical data, together with morphological and electrophysiological data, obtained from the intact sinoatrial node and isolated sinoatrial node cells support the gradient model of the cellular organisation of the SA node. The complex organisation of the sinoatrial node is important for the normal functioning of the sinoatrial node: (i) it allows the sinoatrial node to drive the surrounding hyperpolarized atrial muscle without being suppressed by it; (ii) it helps the pacemaker activity of the sinoatrial node continue under a wide range of physiological and pathophysiological conditions; (iii) it helps protect the sinoatrial node from reentrant arrhythmias.

Key Words: Sinoatrial node, Connexin, Pacemaker activity

INTRODUCTION

The mammalian sinoatrial (SA) node, the pacemaker of the heart, is a complex and inhomogeneous tissue. Most data on the SA node come from the rabbit and this review focuses on the organisation of the rabbit SA node. There are two principal models of the cellular organisation of the rabbit SA node: the gradient and mosaic models. The gradient model was proposed first by Bouman and colleagues (Bleeker et al, 1980) and later by our group (for review see Boyett et al, 2000), whereas the mosaic model was proposed more recently, but also by Bouman and colleagues (Verheijck et al, 1998). According to the gradient model, there is a gradual transition of cell size and type from the centre to the periphery of the SA node. According to the mosaic model, the SA node contains atrial cells as well as SA node cells and the proportion of atrial cells gradually increases from the centre towards the periphery (Boyett et al, 2000). The aim of this review is to discuss whether recent immunocytochemical studies, as well as previous morphological and electrophysiological studies, support the gradient model of the cellular organisation of the rabbit SA node.

Anatomical location of the rabbit SA node

Fig. 1 shows a schematic diagram of a typical SA node preparation from the rabbit after the dissection shown in Fig. 2. In rabbit, the SA node is located in the posterior wall of the right atrium between the entrances of the superior and inferior venae cavae into the right atrium (the region known as the intercaval region). On one side, the SA node is connected to the crista terminalis (CT in Fig. 1), which is a thick band of atrial muscle. In turn, the crista terminalis is connected to the trabeculated atrial muscle of the right atrial appendage (RA in Fig. 1). From the intercaval region, the SA node tissue rises up the endocardial face of the crista terminalis and terminates at the right branch of the sinoatrial ring bundle. On the opposite side of the SA node, the SA node is connected to the atrial septum (SEP in Fig. 1).

Fig. 2 illustrates the dissection of the rabbit SA node and important landmarks that are used to establish the location of the SA node. The right atrium is separated from the ventricles (Fig. 2A), connective tissue (Fig. 2B, C), aorta and pulmonary artery (Fig. 2D) and finally the left atrium (Fig. 2D). The separated right atrium is opened by a longitudinal incision in the anterior wall, between the inferior and superior venae cavae (Fig. 2D, anterior view). The right atrium is then trimmed and the remaining tissue includes the whole SA node and some of the surrounding atrial muscle as shown in Fig. 1. The size of the SA node in rabbit is approximately 4 by 5 mm (Bleeker et al, 1980).

Corresponding to: M.R. Boyett, School of Biomedical Sciences, University of Leeds, Leeds LS2 9JT, UK. (Tel) 44-113-3434298, (Fax) 44-113-3434224, (E-mail) m.r.boyett@leeds.ac.uk

ABBREVIATION: SA, sinoatrial.

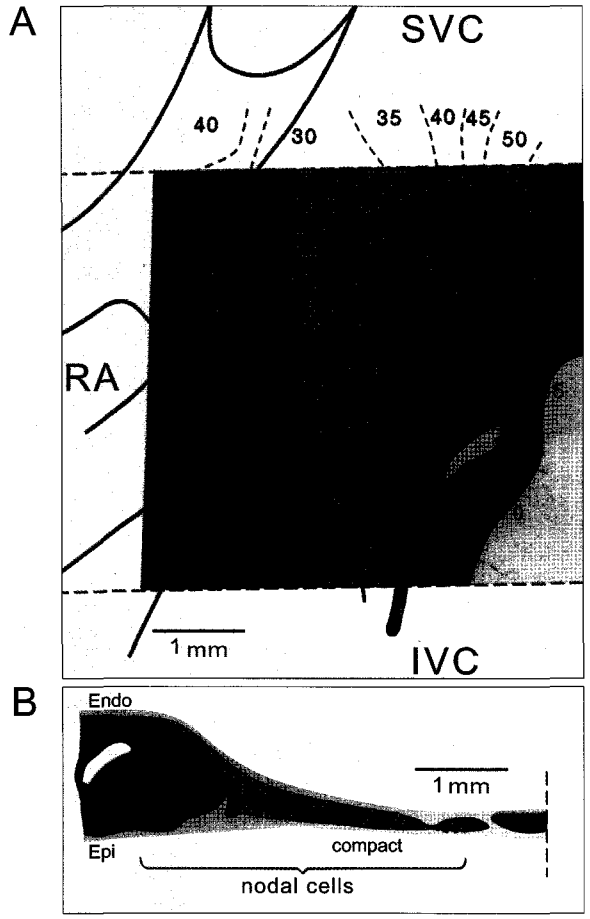

Fig. 1. Histology of the rabbit SA node. A) Schematic diagram of a typical SA node preparation (endocardial view). B) Schematic diagram of a cross section through the crista terminalis and intercaval region. *Position of leading pacemaker site. Isochrones, time (in ms) taken for the action potential to propagate from leading pacemaker site to the area shown. Dark yellow, SA node cells. Dashed yellow line, extent of SA node tissue overlaying the atrial muscle of the crista terminalis. Brown, atrial cells. Pink, no myocardial cells, only connective tissue. Stippled area, interweaving SA node cells. Grey, block zone. SVC, superior vena cava. SEP, interatrial septum. IVC, inferior vena cava. CT, crista terminalis. RA, right atrial appendage. Endo, endocardium. Epi, epicardium. From Boyett et al (2000).

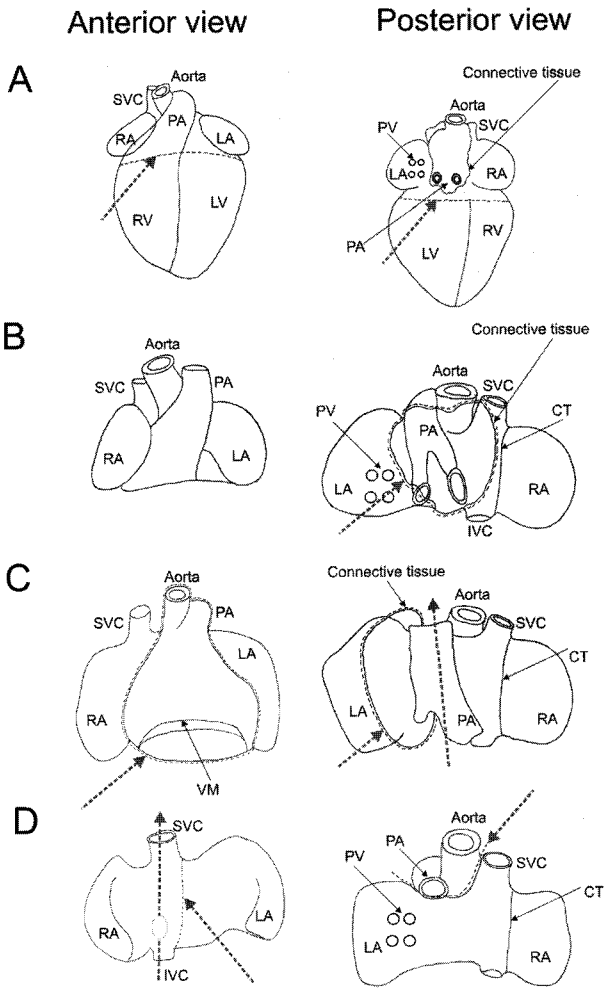

Fig. 2. Dissection of SA node tissue. A) Removal of ventricles along dashed line highlighted by arrow (anterior and posterior view). B) Removal of connective tissue (posterior view). C) Removal of aorta, PA and remaining ventricular muscle (anterior view) and opening of PA and further removal of connective tissue (posterior view). D) Removal of LA and septum (posterior view) and opening of IVC and SVC (anterior view). Dashed line highlighted by arrow, direction of removal of tissue. LA, left atrium. LSARB, left branch of the sinoatrial ring bundle. LV, left ventricle. PA, pulmonary arteries; PV, pulmonary veins; RSARB, right branch of the sinoatrial ring bundle; RV, right ventricle. Other abbreviations are the same as in Fig. 1. From Dobrzynski (2000).

Morphology of the rabbit SA node-histology and ultrastructure

In rabbit, the SA node can be broadly divided into centre and periphery. Histologically, it has been found that typical central SA node cells are small and pale (stained lightly) when compared to working myocardium, and are embedded in connective tissue, mainly collagen fibres and fibroblasts. The extent of connective tissue is 50% in the rabbit (Opthof 1988). Apart from the presence of collagen fibres, the centre of the SA node can be identified as a structure with a high density of nuclei (because the cells are small) and made up of cells irregular in profile and arranged in an 'interweaving' manner (Bleeker et al, 1980; Opthof 1988). Fig. 3A shows a high magnification view of the central SA node area of the rabbit stained with Masson's trichrome - the small interweaving and 'irregular-profile' cells can be seen. The stippled area in Fig. 1 shows the extent of small interweaving cells in the rabbit SA node. Fig. 3B shows a high magnification view of the atrial muscle of the crista terminalis. In comparison to the centre of the SA node (Fig. 3A), the cells in the crista terminalis (Fig. 3B) are regularly arranged and the density of nuclei is lower (because the cells are larger). As shown in Fig. 3A, the SA node in rabbit occupies the entire thickness between the endocardium and epicardium (Bleeker et al, 1980; Opthof et al, 1985).

Ultrastructurally, it has been found that the central SA node cells have a relatively large nucleus, 'empty' cytoplasm

due to a low density of poorly organised myofilaments, low content of sarcoplasmic reticulum and mitochondria and few gap junctions (Opthof et al, 1985). From the centre to the periphery of the SA node, the type, size, shape and arrangement of the cells change. Peripheral SA node cells have a higher density of well-organised myofilaments, higher content of sarcoplasmic reticulum and mitochondria and more numerous gap junctions. Peripheral SA node cells are also larger, more regular in profile and are arranged in parallel with the crista terminalis rather than perpendicular to it (like central SA node cells - Fig. 3A). In Fig. 1, the yellow area (without stipples) shows the region of larger peripheral SA node cells and the dashed yellow line shows the extent of peripheral SA node tissue lying over the atrial muscle of the crista terminalis (brown area). The myofilament content is least in the region of small cells (the stippled area in Fig. 1) and gradually increases in all directions from this region (Boyett et al, 2000). In rabbit, where the periphery of the SA node overlies the atrial muscle of the crista terminalis, the SA node tissue is separated from the atrial muscle of the crista terminalis by connective tissue (Boyett et al, 2000).

Electrophysiology of the intact rabbit SA node - activation sequence and regional differences in action potential properties

At the electrophysiological level, the rabbit SA node can be broadly divided into the primary or leading pacemaker cells (a group of cells with earliest discharge) in the centre of the SA node, and the latent pacemaker cells in the periphery of the SA node. The position of the leading pacemaker site is indicated by the asterisk in Fig. 1. In rabbit, the leading pacemaker site covers an area of 0.1 mm^2 and contains 5,000 cells (~1% of the SA node) and is located in the intercaval region, 0.5 to 2 mm away from the crista terminalis, within the area of small interweaving cells (Fig. 1) (Bleeker et al, 1980). The isochrones in Fig. 1 show the time (in ms) taken for the action potential to propagate from the leading pacemaker site. From the leading pacemaker site, the action potential propagates in an oblique cranial direction towards the crista terminalis and then into the atrial muscle and from here it propagates to the rest of the heart. Close to the leading pacemaker site, in the centre of the SA node, the action potential is conducted at a velocity of 4.5 cm/s roughly parallel to the crista terminalis and 3.0 cm/s perpendicular to it (Yamamoto et al, 1998). In the periphery of the SA node, the action potential is conducted more rapidly at a velocity of 49.7 cm/s roughly parallel to the crista terminalis and 36.3 cm/s perpendicular to it (Yamamoto et al, 1998). In the rabbit SA node, there is also a block zone (the thick grey line in Fig. 1A). In the block zone, conduction is blocked and aborted action potentials can be observed.

As in the case of morphology, in the rabbit SA node there are regional differences in the action potential configuration (Bleeker et al, 1980; Boyett et al, 2000). In the centre of the SA node, the upstroke of the action potential is low (<10 V/s), the action potential overshoot is low (<10 mV), the action potential is long (~150 ms), the maximum diastolic potential is low (−60 to −70 mV) and the pacemaker potential is steep. From the centre to the periphery of the SA node, there is a gradual increase in action potential amplitude, maximum diastolic potential, maximum upstroke velocity and action potential overshoot, and gradual decreases in action potential duration and steepness of the pacemaker potential. The action potential duration is greatest at or near the leading pacemaker site.

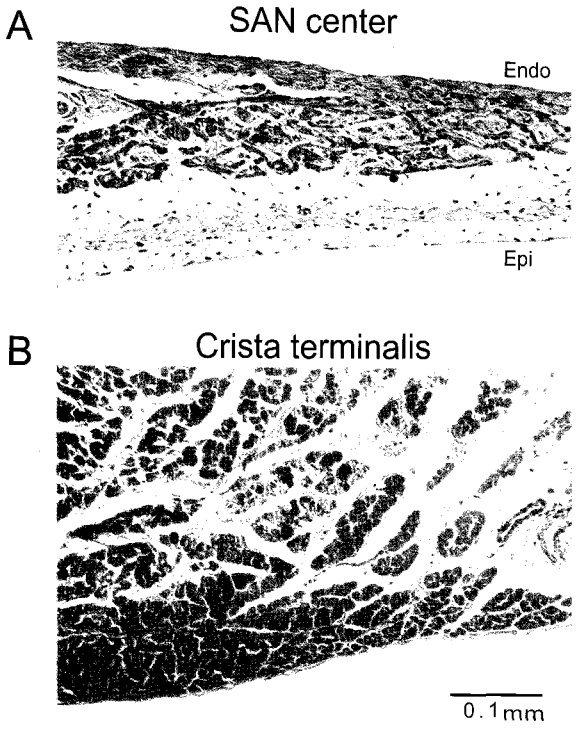

Fig. 3. Light microscope views of transversely cut sections through the centre of the SA node and the atrial muscle of the crista terminalis of the rabbit stained with Masson's trichrome. A) Centre of the SA node. B) Atrial muscle of the crista terminalis. From Dobrzynski (2000).

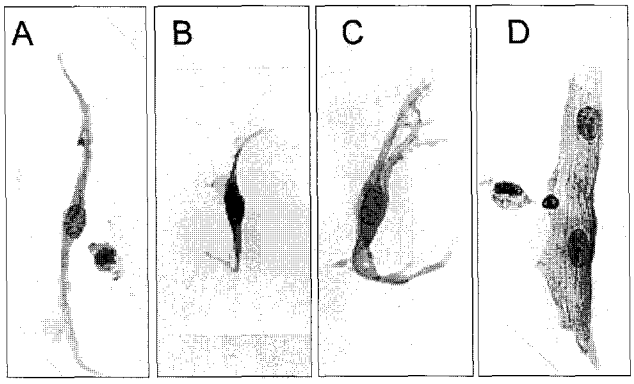

Fig. 4. Morphology of different cell types isolated from a rabbit SA node-atrial muscle preparation and stained with haematoxylin and eosin. A) Elongated spindle-shaped cell. B) Spindle-shaped cell. C) Spider-shaped cell. D) Atrial cell. Scale bar 30 μm. From Verheijck et al (1998).

Morphological and electrical properties of single rabbit SA node cells

Fig. 4 illustrates the morphology of different cell types observed in the rabbit SA node. Following enzymatic isolation, three morphologically different cell types are observed in the SA node: irregular spindle-shaped cells (Fig. 4B) with a diameter of less than ~8 μm and length of 20~35 μm (found predominantly in the centre of the SA node), elongated spindle-shaped cells (Fig. 4A) with a length of 50~80 μm and spider-shaped cells (Fig. 4C) with multiple cytoplasmic projections (Denyer & Brown, 1990; Verheijck, 1994; Verheijck et al, 1998; Wu et al, 2001). In contrast, atrial cells (Fig. 4D) are more rectangular in shape with a diameter of 15~20 and length of ~100 μm. Verheijck et al (1998) also observed atrial cells in the SA node.

Fig. 5 shows dimensions of rabbit SA node cells. Using confocal microscopy to measure dimensions of pacemaker cells, M. Lei (unpublished data) showed that cells isolated from the centre of the SA node are small (length, ~51 μm, Fig. 5A; width ~10 μm, Fig. 5C) and non-striated, while cells isolated from the periphery of the SA node are significantly larger in terms of length (~88 μm, Fig. 5B), but not in terms of width (Fig. 5D), and 38% of them are striated. Unlike Verheijck et al, (1998), M. Lei did not observe a significant number of atrial cells amongst cells isolated from the SA node.

Fig. 6 shows the relationship between electrical activity and the size of rabbit SA node cells as measured by cell capacitance, C_m, from the study of Honjo et al (1996). In their study, SA node cells of different size showed different action potential configurations. Take-off potential, maximum upstroke velocity, action potential amplitude and maximum diastolic potential were significantly correlated with C_m; these parameters were greater in larger cells (presumably from the periphery of the SA node; Fig. 6). For example, relatively small SA node cells with $C_m < 30$ pF had a maximum upstroke velocity of 10 V/s or less, whereas some larger cells had a maximum upstroke velocity of >60 V/s. The slope of the pacemaker potential and cycle length were also correlated significantly with C_m; the pacemaker potential was less steep and intrinsic spontaneous activity was slower in smaller cells (presumably from the centre of the SA node; Fig. 6). The data in Fig. 6 suggest that the regional differences in the action potential in the intact SA node are the result of regional differences in the intrinsic properties of the cells (Honjo et al, 1996). Verheijck and colleagues (Verheijck 1994; Verheijck et al, 1998), on the other hand, reported that although the electrical activity of SA node is inhomogeneous, there is no correlation with cell type (e.g. morphologically identical cells can show markedly different electrical activity). Partly because of this, they suggested that the gradual transition of electrical activity from the centre to the periphery of the SA node is the result of a gradual increase in the ratio of atrial cells:SA node cells from the centre to the periphery.

Gradient versus mosaic models of cellular organisation of the rabbit SA node

Fig. 7 shows the gradient and mosaic models of the

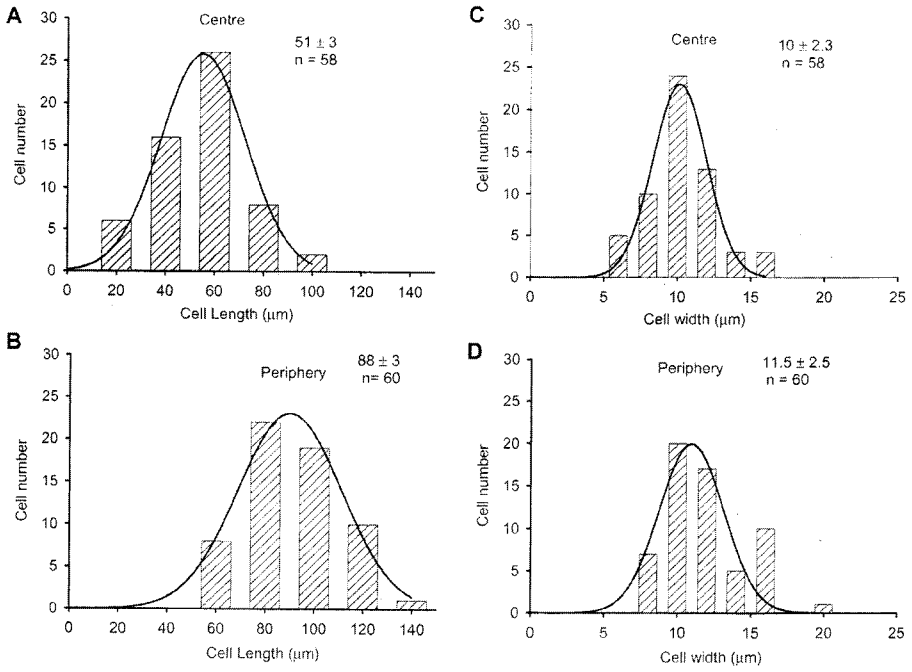

Fig. 5. Dimensions of SA node cells isolated from different regions of the rabbit SA node measured using confocal microscopy. A) Length of central SA node cells. B) Length of peripheral SA node cells. C) Width of central SA node cells. D) Width of peripheral SA node cells. Means ± SEM and n number given. From M. Lei (unpublished data).

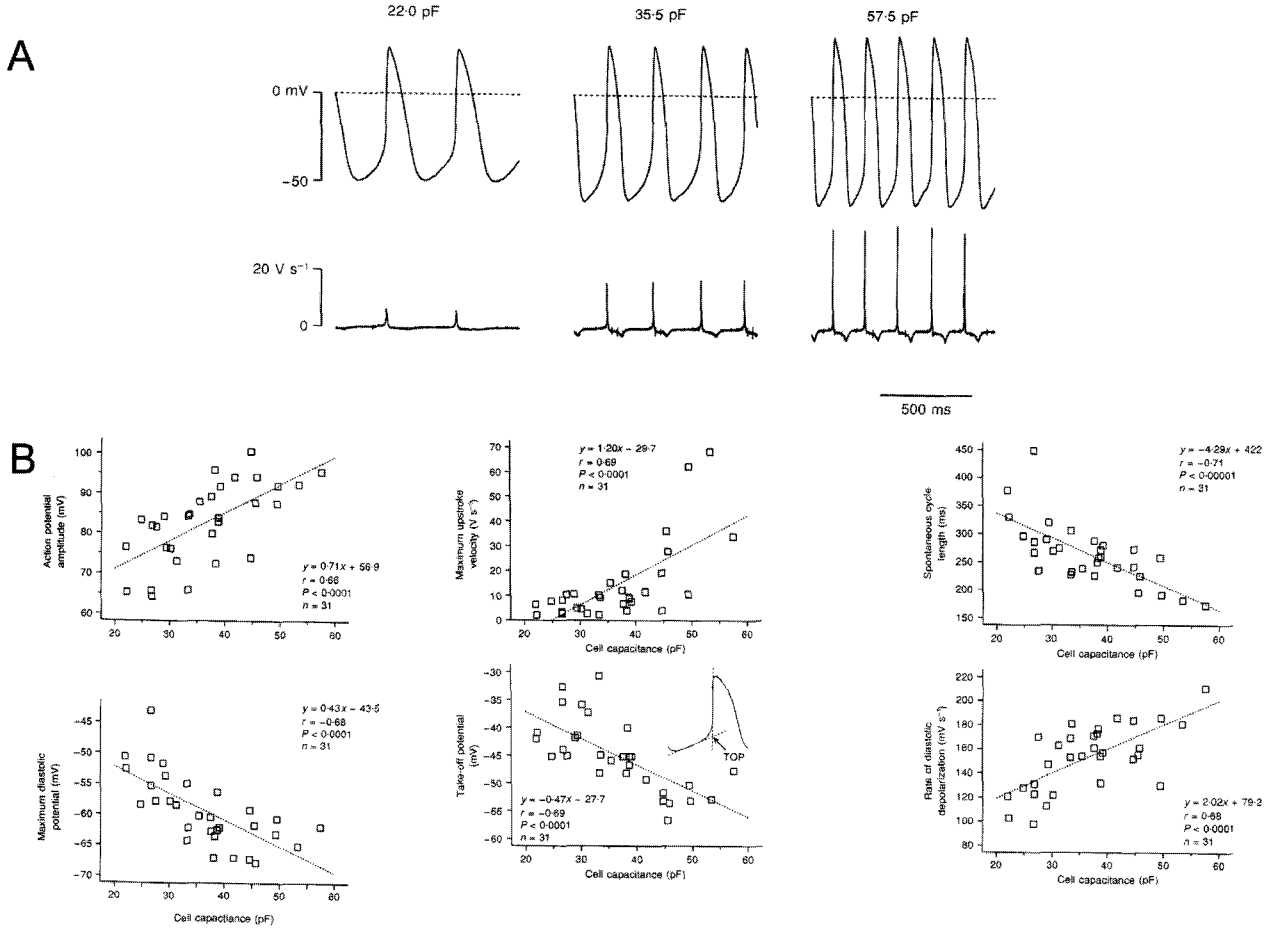

Fig. 6. A) Spontaneous action potentials recorded from three rabbit SA node cells of different size. Top, membrane potential. Bottom, rate of change of membrane potential. C_m shown above each record. B) Correlation between action potential parameters and the size of rabbit SA node cells. Six action potential parameters are plotted against C_m. The dotted lines were fitted by linear regression. The results of the linear regression are shown. From Honjo et al (1996).

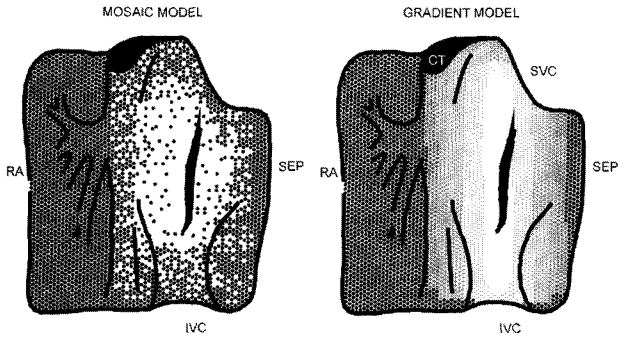

Fig. 7. Gradient and mosaic models of the cellular organisation of the rabbit SA node. Left, mosaic model characterised by mixture of SA node (white) and atrial (black) cells. Right, gradient model characterised by gradual morphological transition of cell type from the centre (white) through periphery (grey) of the SA node to the surrounding atrial muscle (black). Vertical black area on the septal side of the centre of the SA node: block zone. Abbreviations are the same as in Fig. 1. From Boyett et al (2000).

cellular organisation of the rabbit SA node. According to the gradient model there is a gradual transition of SA node cell size and type from the centre to the periphery of the SA node. The size of pacemaker cells gradually increases from the centre to the periphery of the SA node (Fig. 5) (Bleeker et al, 1980; Boyett et al, 2000). According to the gradient model, action potential characteristics and ionic current densities vary in a similar way to cell size (Boyett et al, 2000). The regional differences in the action potential (discussed in section 5.2) are presumed to be the result of regional differences in the intrinsic properties of the cells (i.e. ionic current densities).

According to the mosaic model (Fig. 7) there is a random mix of morphologically different cell types, i.e. SA node and atrial cells (see Fig. 4), in all regions of the SA node (as observed by Verheijck et al, 1998), and the density of atrial cells gradually increases from the centre towards the periphery of the SA node (Verheijck et al, 1998). The estimated ratio of atrial cells : SA node cells in the centre of the SA node is 41 : 59 and in the periphery of the SA node is 63 : 27 (Verheijck et al, 1998). In addition, according to the mosaic model, morphological differences in SA node cells are not associated with differences in action

potential configuration and pacemaker activity (contrary to the gradient model). Therefore, the mosaic model proposes that the regional differences in electrical activity in the SA node are not the result of a gradient in the intrinsic properties of SA node cells from the centre to the periphery - instead they are the result of variation in the proportions of atrial and SA node cells from the centre to the periphery (Verheijck et al, 1998).

Our observations on single cells isolated from the rabbit SA node support the gradient model, because, firstly, we do not observe a significant number of atrial cells amongst cells isolated from the SA node and, secondly, we do find that morphological differences in SA node cells are associated with differences in action potential configuration and pacemaker activity (Fig. 6). The next section will review recent immunocytochemical evidence for the gradient model of the cellular organisation of the rabbit SA node.

Immunocytochemical evidence for the gradient model of the cellular organisation of the rabbit SA node

Connexins - Cx43, Cx45 and Cx40

In order to maintain normal function, the SA node requires a fine balance of electrical coupling (Joyner & van Capelle, 1986). The SA node has to be electrically connected to the atrial muscle to be able to drive it, but the coupling must not be strong, because the atrial muscle, which acts as a hyperpolarizing load on the SA node, will cause the spontaneous activity of the SA node to stop (Joyner & van Capelle, 1986). Connexins, a multiple family of conserved proteins, make up the gap junctions responsible for electrical coupling (Severs, 1990). Immunocytochemical studies have revealed that Cx43 is the most abundant connexin in the working myocardium (atrial and ventricular muscle) but is negligible in the conducting tissues of the heart (Coppen et al, 1999). However, ultrastructual studies have showed the presence of gap junctions in the SA node of rabbit as well as in other mammalian species (Opthof, 1994) and immunocytochemical studies have shown other connexin subtypes in the SA node (Boyett et al, 2000).

Fig. 8A shows a schematic diagram of the distribution of three different connexin subtypes in the rabbit SA node. The centre of the SA node in the intercaval region lacks Cx43 expression (white area in Fig. 8A), but Cx40 and Cx45 are expressed in the Cx43 negative area (Coppen et al, 1999). From the intercaval region, peripheral SA node tissue rises up the endocardial face of the crista terminalis, where it terminates. The periphery of the SA node expresses both Cx43 as well as Cx45 (yellow area in Fig. 8A). The bulk of the crista terminals is atrial muscle which contains Cx43 (grey area in Fig. 8A). As an example, Fig. 8B shows a tissue section cut through the crista terminalis and intercaval region of rabbit labelled for Cx43. The expression of Cx43 in the periphery, but not in the centre of the SA node, can be seen.

In the immunocytochemical study of Coppen et al (1999), on intact rabbit SA node tissue sections, it was not possible to elucidate the relationship between SA node cell morphology and expression of connexin subtypes, because tissue sections were used. However, our recent study on cells isolated from the rabbit SA node showed that there is a clear cell size-dependence in pattern of connexin subtype expression (Honjo et al, 2002). Fig. 9 shows two different connexin subtypes expressed in SA node cells (Honjo et al, 2002). Immunofluorescent spots for Cx43 were negligible in small irregular spindle-shaped (Fig. 9A) and spider-shaped SA node cells (Fig. 9B), presumably from the centre of the SA node. In contrast, small immunofluorescent spots for Cx43 were detected over the cell surface membrane in some large spindle-shaped cells (Fig. 9E), presumably from the periphery of the SA node. Immunofluorescent spots for Cx45 of varying density were detected over the cell surface membrane in small spider-shaped (Fig. 9C, D) and large spindle-shaped cells (Fig. 9F). Fig. 9G, H summarises these data: the density of Cx43 (Fig. 9G) and Cx45 (Fig. 9H) labelling is plotted against the size of isolated SA node cells. The density of Cx43 labelling was higher in larger SA node cells, but lower than in atrial cells, and the density of Cx45 labelling was higher in smaller SA node cells. Cx45 labelling was absent in atrial cells. These results from single SA node cells (Honjo et al, 2002) are in accord with our previous study on SA node tissue sections (Coppen et al, 1999). Coppen et al (1999) showed that Cx45, as well as Cx40, but not Cx43, is expressed in the centre of the SA node, whereas both Cx43 and Cx45 are expressed in the periphery of the SA node (Fig. 8A), and Honjo et al (2002) showed that small irregular spindle-shaped and spider shaped cells (presumably derived from the centre of the SA node) express Cx45, but not Cx43 and large spindle-shaped SA node cells (presumably from the periphery of the SA node) expressed both Cx43 and Cx45 (Fig. 9).

These results are consistent with the gradient model of the rabbit SA node. Verheule et al (2001) also investigated the correlation between cell morphology and connexin subtypes in the rabbit SA node and showed that Cx43 is absent in small spindle- and spider-shaped cells, but present in elongated spindle-shaped cells. These results are

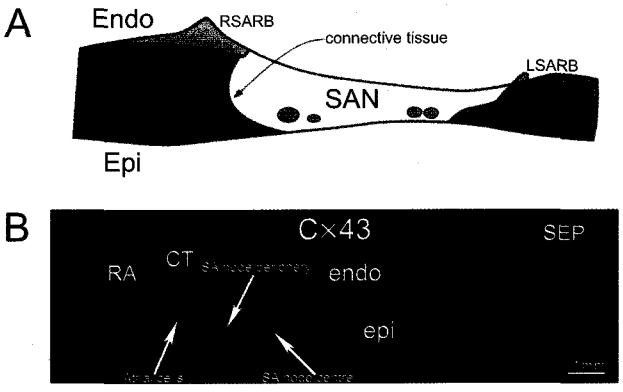

Fig. 8. A) Schematic diagram showing distribution of connexin subtypes in the rabbit SA node. The diagram shows the distribution of Cx40, Cx43 and Cx45 in a section through the crista terminalis and the intercaval region. White area: area of Cx40 and Cx45 but not Cx43 expression. Yellow area: area of Cx43 and Cx45 expression. Grey area: area of Cx43 expression. Black area: connective tissue separating SA node tissue from atrial muscle of crista terminalis. From Coppen et al (1999). B) Section through the atrial muscle of the crista terminalis and the intercaval region labelled for Cx43. Scale bar 1 mm. From Musa et al (2002). Abbreviations are the same as in Fig. 1.

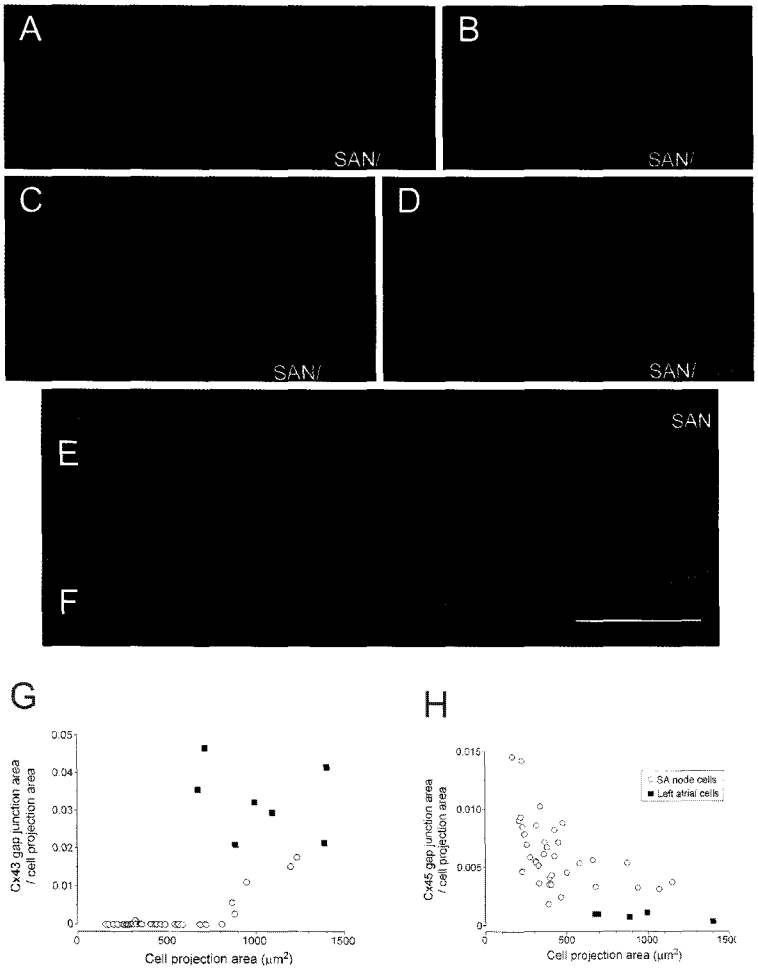

Fig. 9. A, B) No Cx43 labelling in small spindle-shaped SA node (A) and spider-shaped SA node (B) cells. C, D) Cx45 labelling in spider-shaped cells. E) Cx43 labelling in a large spindle-shaped SA node cell. F) Cx45 labelling in a large spindle-shaped SA node cell. G, H) Correlation between density of Cx43 (G) and Cx45 (H) immunolabelling and cell size. Area of cell labelled with Cx43 and Cx45 antibody (calculated from projection image), normalised for cell projection area, is plotted against cell projection area. Open circles, data for SA node cells. Filled squares, data for left atrial cells. Scale bar, 20 μm. From Honjo et al (2001).

consistent with those of Coppen et al (1999) & Honjo et al (2001).

We have recently shown that Cx43 mRNA as well as Cx43 protein is absent from the rat SA node and therefore, the lack of Cx43 protein in the SA node is the result of a lack of transcription.

L-type Ca^{2+} channel and Na^{+}-Ca^{2+} exchanger

Ca^{2+} is important in the SA node. The L-type Ca^{2+} current, $i_{Ca,L}$, supports the action potential and pacemaker activity and there is now evidence that Ca^{2+} release from the sarcoplasmic reticulum (SR) is involved in pacemaking by affecting other ionic currents, e.g. Na^{+}-Ca^{2+} exchanger current (Hata et al, 1996; Rigg & Terrar, 1996). The densities of various ionic currents are significantly correlated with the size of rabbit SA node cells as measured by the cell capacitance, C_m (Boyett et al, 2000). Fig. 10A shows a plot of the density of $i_{Ca,L}$ at 0 mV against C_m (Musa et al, 2002). In Fig. 10A, the density of $i_{Ca,L}$ is significantly ($P < 0.001$) correlated with C_m and the density was greater in larger SA node cells (likely to be from the periphery of the SA node) than in smaller SA node cells (likely to be from the centre of the SA node). Computer models of the action potential of the SA node in the centre and periphery estimated that in the centre of the SA node the density if $i_{Ca,L}$ should be ~30% of that in the periphery of the SA node (Zhang et al, 2000): this is in accord with the experimental measurements (Fig. 10A). Our recent immunocytochemical study (Musa et al, 2002) showed that L-type Ca^{2+} channel as well as Na^{+}-Ca^{2+} exchanger labelling varied in cells isolated from different regions of the rabbit

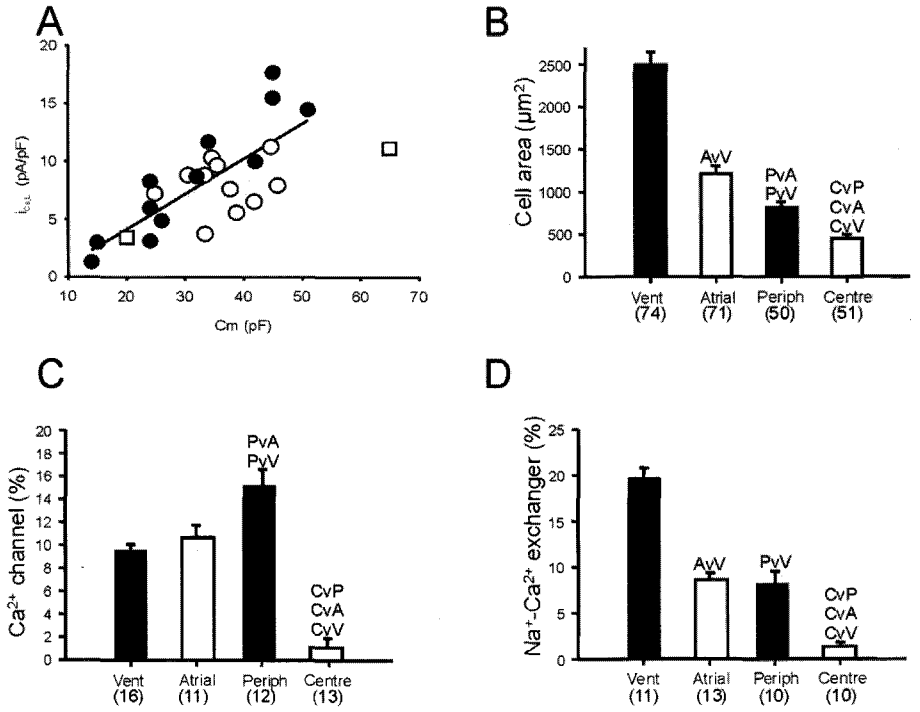

Fig. 10. A) Correlation between $i_{Ca,L}$ density and C_m. Plot of density of $i_{Ca,L}$ at 0 mV against C_m for different cells isolated from rabbit SA node is shown. From Musa et al (2000). See Musa et al (Musa et al, 2002) for meaning of different symbols. B) Mean (±SEM) area of ventricular, atrial, peripheral SA node and central SA node cells. C, D) Mean (±SEM) density of labelling of L-type of Ca^{2+} channel (C) and Na^+-Ca^{2+} exchanger (D) of ventricular, atrial, peripheral SA node and central SA node cells. From Musa et al (2002). All data from rabbit.

SA node. In study of Musa et al (2002) the cells were separately isolated from tissue taken from the centre and the periphery of the SA node. Fig. 11 shows single cells isolated from the centre (Fig. 11A, B) and periphery (Fig. 11C, D) of the SA node labelled for the L-type Ca^{2+} channel (Fig. 11A, C) as well as the Na^+-Ca^{2+} exchanger (Fig. 11B, D). In peripheral SA node cells, there was L-type Ca^{2+} channel (Fig. 11C) as well as Na^+-Ca^{2+} exchanger (Fig. 11D) labelling at the surface cell membrane, whereas in the central SA node cells there was little or no detectable labelling of either the L-type Ca^{2+} channel (Fig. 11A) or the Na^+-Ca^{2+} exchanger (Fig. 11B). Image analysis was used to measure the total area of labelling within an optical section approximately midway through the depth of a cell as well as the total area of the cell in the optical section, from which the density of labelling (percentage of cell area labelled) was calculated. Fig. 10 shows the density of labelling of the L-type Ca^{2+} channel (Fig. 10C) as well as the Na^+-Ca^{2+} exchanger (Fig. 10D) in SA node, atrial and ventricular cells. The density of L-type Ca^{2+} channel (Fig. 10C) as well as Na^+-Ca^{2+} exchanger (Fig. 10D) labelling was high in atrial and peripheral SA node cells, but significantly less in central SA node cells - this is consistent with electrophysiological data (Fig. 10A). It is also interesting that in the study of Musa et al, (2002) the density of other Ca^{2+} handling proteins (RYR2 and SERCA2) was also significantly less in central than peripheral SA node cells. Fig. 10B shows that as expected the area of peripheral SA node cells is greater than that of central SA node cells.

As with the studies on connexin subtype expression in

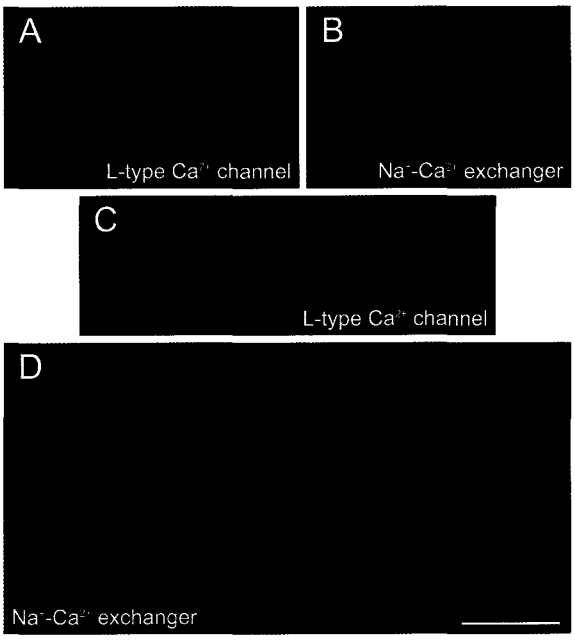

Fig. 11. A) No L-type Ca^{2+} channel labelling in a small spindle-shaped SA node cell. B) No Na^+-Ca^{2+} exchanger labelling in a small spider-shaped SA node cell. C, D) L-type Ca^{2+} channel (C) and Na^+-Ca^{2+} exchanger (D) labelling in peripheral SA node cells. The nucleus is stained red by propidium iodide in panel A. Scale bar, 20 μm. From Musa et al (2002).

SA node cells discussed above, Musa et al (2002) therefore showed a clear correlation between L-type Ca^{2+} channel and Na^{+}-Ca^{2-} exchanger expression and the cell type within the SA node. Once again this is consistent with the gradient model of the rabbit SA node.

CONCLUSIONS

There is considerable interest in how the SA node is organised (Verheijck et al, 1998; Boyett et al, 2000). Two possibilities are the gradient and mosaic models. The recent immunocytochemical studies presented in this review (together with morphological and electrophysiological studies) obtained from the intact SA node and isolated SA node cells support the gradient model of the cellular organisation of the rabbit SA node (Coppen et al, 1999; Honjo et al, 2001; Musa et al, 2002). A mathematical modelling study of the gradient and mosaic models also favoured the gradient model (Zhang et al, 2001). It is concluded, therefore, that the current evidence supports the gradient rather than the mosaic model of the cellular organisation of the rabbit SA node.

This complex and heterogeneous organisation of the SA node is important for the normal functioning of the SA node: (i) it helps the SA node drive the more hyperpolarized surrounding atrial muscle and not be suppressed by it; (ii) it helps the pacemaker activity of the SA node continue under a wide range of physiological and pathophysiological conditions; (iii) it helps protect the SA node from reentrant arrhythmias (Boyett et al, 2000).

REFERENCES

Bleeker WK, Mackaay AJC, Masson-Pevet M, Bouman LN, Becker AE. Functional and morphological organization of the rabbit sinus node. *Circ Res* 46: 11–22, 1980.

Boyett MR, Honjo H, Kodama I. The sinoatrial node, a heterogeneous pacemaker structure. *Cardiovasc Res* 47: 658–687, 2000.

Coppen SR, Kodama I, Boyett MR, Dobrzynski H, Takagishi Y, Honjo H, Yeh H-I, Severs NJ. Connexin45, a major connexin of the rabbit sinoatrial node, is co-expressed with connexin 43 in a restricted zone at the nodal-crista terminalis border. *J Histochem Cytochem* 47: 907–918, 1999.

Denyer JC, Brown HF. Rabbit sino-atrial node cells: isolation and electrophysiological properties. *J Physiol* 428: 405–424, 1990.

Dobrzynski H. Immunocytochemical localisation of K^{+} channels in the sinoatrial node. University of Leeds. Ph.D. thesis, 2000.

Hata T, Noda T, Nishimura M, Watanabe Y. The role of Ca^{2+} release from sarcoplasmic reticulum in the regulation of sinoatrial node automaticity. *Heart Vessels* 11: 234–241, 1996.

Honjo H, Boyett MR, Coppen SR, Takagishi Y, OpThof T, Severs NJ, Kodama I. Heterogeneous expression of connexins in rabbit sinoatrial node cells: correlation between connexin isotype and cell size. *Cardiovasc Res* 53: 89–96, 2002.

Honjo H, Boyett MR, Kodama I, Toyama J. Correlation between electrical activity and the size of rabbit sinoatrial node cells. *J Physiol* 496: 795–808, 1996.

Joyner RW, Van Capelle FJL. Propagation through electrically coupled cells: how a small SA node drives a large atrium. *Biophys J* 50: 1157–1164, 1986.

Kodama I, Boyett MR. Regional differences in the electrical activity of the rabbit sinus node. *Pflügers Arch* 404: 214–226, 1985.

Musa H, Lei M, Honjo H, Jones SA, Dobrzynski H, Takagishi Y, Henderson Z, Kodama I, Boyett MR. Heterogeneous expression of Ca^{2+} handling proteins in sinoatrial node. *J Histochem Cytochem* 50: 311–324, 2001.

OpThof T. The mammalian sinoatrial node. *Cardiovasc Drugs Therapy* 1: 573–597, 1988.

OpThof T. Gap junctions in the sinoatrial node: immunohistochemical localization and correlation with activation patterns. *J Cardiovasc Electrophysiol* 5: 138–143, 1994.

OpThof T, De Jonge B, Mackaay AJC, Bleeker WK, Masson-Pevet M, Jongsma HJ, Bouman LN. Functional and morphological organization of the guinea-pig sinoatrial node compared with the rabbit sinoatrial node. *J Mol Cell Cardiol* 17: 549–564, 1985.

Rigg L, Terra DA. Possible role of calcium release from the sarcoplasmic reticulum in pacemaking in guinea-pig sino-atrial node. *Exp Physiol* 81: 877–880, 1996.

Severs NJ. The cardiac gap junctions and intercalated disc. *Int J Cardiol* 26: 137–173, 1990.

Ten Velde I, De Jonge B, Verheijck EE, Van Kempen MJA, Analbers L, Gros D, Jongsma HJ. Spatial distribution of connexin43, the major cardiac gap junction protein, visualizes the cellular network for impulse propagation from sinoatrial node to atrium. *Circ Res* 76: 802–811, 1995.

Verheijck EE. Pacemaker currents in the sino-atrial node. University of Amsterdam. Ph.D. thesis, 1994.

Verheijck EE, Wessels A, Van Ginneken ACG, Bourier J, Markman MWM, Vermeulen JLM, De Bakker JMT, Lamers WH, OpThof T, Bouman LN. Distribution of atrial and nodal cells within rabbit sinoatrial node. Models of sinoatrial transition. *Circulation* 97: 1623–1631, 1998.

Verheule S, Van Kempen MJA, Postma S, Rook MB, Jongsma HJ. Gap Junctions in the rabbit sinoatrial node. *Am J Physiol* 280: H2103–H2115, 2001.

Wu J, Schuessler RB, Rodefeld MD, Saffitz JE, Boineau JP. Morphological and membrane characteristics of spider and spindle cells isolated from rabbit sinus node. *Am J Physiol* 280: H1232–H1240, 2001.

Yamamoto M, Honjo H, Niwa R, Kodama I. Low frequency extracellular potentials recorded from the sinoatrial node. *Cardiovas Res* 39: 360–372, 1998.

Zhang H, Holden AV, Boyett MR. A gradient model of the intact SA node-initiation and propagation of pacemaker activity. *Circulation* 103: 584–588, 2001.

Zhang H, Holden AV, Kodama I, Honjo H, Lei M, Varghese T, Boyett MR. Mathematical models of action potentials in the periphery and center of the rabbit sinoatrial node. *Am J Physiol* 279: H397–H421, 2000.